Neurobiology of Disease 64 (2014) 48–59

Contents lists available at ScienceDirect

Neurobiology of Disease

journal homepage: www.elsevier.com/locate/ynbdi

Knocking down metabotropic glutamate receptor 1 improves survival and disease progression in the *SOD1^{G93A}* mouse model of amyotrophic lateral sclerosis ☆

Marco Milanese [a], Francesco Giribaldi [a], Marcello Melone [b,c], Tiziana Bonifacino [a], Ilaria Musante [d,e], Enrico Carminati [f], Pia I.A. Rossi [d,e], Laura Vergani [f], Adriana Voci [f], Fiorenzo Conti [b,c], Aldamaria Puliti [d,e,1], Giambattista Bonanno [a,*,1]

[a] Department of Pharmacy, Unit of Pharmacology and Toxicology and Center of Excellence for Biomedical Research, University of Genoa, Genoa, Italy
[b] Department of Experimental and Clinical Medicine, Unit of Neuroscience and Cell Biology, Università Politecnica delle Marche, Ancona, Italy
[c] Center for Neurobiology of Aging, INRCA IRCCS, Ancona, Italy
[d] Department of Neuroscience, Rehabilitation, Ophthalmology, Genetics and Maternal and Child Health, Medical Genetics Unit, University of Genoa, Genoa, Italy
[e] Medical Genetics Unit, Istituto Giannina Gaslini, Genoa, Italy
[f] Department of Earth, Environment and Life Sciences, University of Genoa, Genoa Italy

ARTICLE INFO

Article history:
Received 31 July 2013
Revised 17 October 2013
Accepted 12 November 2013
Available online 19 December 2013

Keywords:
Amyotrophic lateral sclerosis
SOD1^{G93A} mouse
Metabotropic glutamate type 1 receptor
Metabotropic glutamate type 5 receptor
Metabotropic glutamate type 1 receptor knocking down
Glutamate transmission
Disease development

ABSTRACT

Amyotrophic lateral sclerosis (ALS) is a late-onset fatal neurodegenerative disease reflecting degeneration of upper and lower motoneurons (MNs). The cause of ALS and the mechanisms of neuronal death are still largely obscure, thus impairing the establishment of efficacious therapies. Glutamate (Glu)-mediated excitotoxicity plays a major role in MN degeneration in ALS. We recently demonstrated that the activation of Group I metabotropic Glu autoreceptors, belonging to both type 1 and type 5 receptors (mGluR1 and mGluR5), at glutamatergic spinal cord nerve terminals, produces excessive Glu release in mice over-expressing human superoxide-dismutase carrying the G93A point mutation (*SOD1^{G93A}*), a widely used animal model of human ALS. To establish whether these receptors are implicated in ALS, we generated mice expressing half dosage of mGluR1 in the *SOD1^{G93A}* background (*SOD1^{G93A}Grm1$^{crv4/+}$*), by crossing the *SOD1^{G93A}* mutant mouse with the *Grm1$^{crv4/+}$* mouse, lacking mGluR1 because of a spontaneous recessive mutation. *SOD1^{G93A}Grm1$^{crv4/+}$* mice showed prolonged survival probability, delayed pathology onset, slower disease progression and improved motor performances compared to *SOD1^{G93A}* mice. These effects were associated to reduction of mGluR5 expression, enhanced number of MNs, decreased astrocyte and microglia activation, normalization of metallothionein and catalase mRNA expression, reduced mitochondrial damage, and decrease of abnormal Glu release in spinal cord of *SOD1^{G93A}Grm1$^{crv4/+}$* compared to *SOD1^{G93A}* mice. These results demonstrate that a lower constitutive level of mGluR1 has a significant positive impact on mice with experimental ALS, thus providing the rationale for future pharmacological approaches to ALS by selectively blocking Group I metabotropic Glu receptors.

Introduction

Amyotrophic lateral sclerosis (ALS) is a progressive neuromuscular disorder characterized by degeneration of cortical, brainstem and spinal motoneurons (MNs) leading to muscle wasting, weakness and spasticity. ALS has an incidence of approximately 1–2 new cases per 100,000 individuals every year and is most commonly sporadic, although familial forms have been reported in about 10% of cases (Andersen and Al-Chalabi, 2011). The first identified ALS-linked gene is the superoxide dismutase-1 (SOD1) that accounts for about 20% of patients with familial ALS (Birve et al., 2010; Rosen et al., 1993). So far, at least other fifteen genes involved in different cellular pathways have been associated to ALS, thus indicating that, even though pathogenic mechanisms are still elusive, multiple cellular events contribute to the disease (Andersen and Al-Chalabi, 2011). These events include oxidative stress,

Abbreviations: ALS, amyotrophic lateral sclerosis; AMPA, α-amino-3-hydroxy-5-methyl-4-isoxazole propionate; [^{3}H]D-Asp, [^{3}H]D-aspartate; CAT, catalase; 3,5-DHPG, (S)-3,5-dihydroxyphenylglycine; Gapdh, Glyceraldehyde 3-phosphate dehydrogenase; Glu, glutamate; LTR, long terminal repeat; mGluR1, metabotropic glutamate receptor 1; mGluR5, metabotropic glutamate receptor 5; MN, motoneuron; MT, metallothionein; NMDA, N-methyl-D-aspartate; PB, phosphate buffer; PFA, paraformaldehyde.

* Corresponding author at: Department of Pharmacy, Unit of Pharmacology and Toxicology, University of Genoa, Viale Cembrano 4, 16148 Genoa, Italy. Fax: +39 010 3993360.
E-mail address: bonanno@pharmatox.unige.it (G. Bonanno).

Available online on ScienceDirect (www.sciencedirect.com).

[1] Equal contribution.

0969-9961/$ – see front matter © 2013 The Authors. Published by Elsevier Inc. All rights reserved.
http://dx.doi.org/10.1016/j.nbd.2013.11.006

mitochondrial dysfunction, protein aggregation, impaired anterograde and retrograde transport, neuroinflammation, dysregulated RNA signaling, and glutamate(Glu)-mediated excitotoxicity (Cleveland et al., 1996; Ferraiuolo et al., 2011).

Glu exerts its actions through activation of ionotropic and metabotropic receptors. Three ionotropic receptor families, namely the Ca^{2+}-permeant N-methyl-D-aspartate (NMDA) receptor, and the preferentially Na^{+}-permeant α-amino-3-hydroxy-5-methyl-4-isoxazole propionate (AMPA) and kainate receptors, exist as multiple heteromers formed by the co-assembly of different subunits (Conti and Weinberg, 1999; Dingledine et al., 1999). Metabotropic glutamate receptors (mGluR) are also heterogeneous and classified into three groups, based on their sequence homology, signaling and pharmacology (Conn and Pin, 1997; Nicoletti et al., 2011). Group I mGluRs, comprising mGluR1 and mGluR5, are excitatory because of positive coupling to phosphatidylinositol breakdown (Conn and Pin, 1997; De Blasi et al., 2001; Ferraguti et al., 2008). Thus, hyper-activation of Glu receptors may lead to an excessive increase of intracellular calcium due to either its entry through ionotropic Glu receptors and/or to its release from intracellular stores, mediated by Group I mGluRs and contributing to excitotoxicity and cell death (Doble, 1999).

Evidence implicating Glu-mediated excitotoxicity in ALS is mainly based on the presence of elevated levels of extracellular Glu in a high percentage of sporadic and familial ALS patients (Perry et al., 1990), on the reduced expression of the Glu transporter type 1 (GLT1) in the affected areas of the CNS (Rothstein et al., 1992, 1995) and on the observation that ameliorating excitotoxicity is to date the only clinically-adopted strategy to slow down disease progression in ALS (Cheah et al., 2010).

The molecular mechanisms of MN degeneration in ALS have been largely investigated in the subtype of disease caused by SOD1 mutations. Mouse models expressing mutated SOD1 reproduce most of the pathogenic processes underlying human ALS, including unfolded protein response activation (Wang et al., 2011a), altered AMPA receptor subunit expression (Tortarolo et al., 2006), reduced expression and activity of GLT1 (Boston-Howes et al., 2006), loss of astrocytic regulation GluR2 expression in MNs (Van Damme et al., 2007), impaired calcium buffering in mitochondria (Damiano et al., 2006) defective axonal transport (Bilsland et al., 2010), and Glu mediated excitotoxicity (Heath and Shaw, 2002). In addition, our recent studies with mice expressing human SOD1 carrying the G93A point mutation ($SOD1^{G93A}$), the most widely used animal model for human ALS, indicate that Glu release is abnormally high in the spinal cord of these animals upon exposure to different releasing stimuli, including nerve terminal depolarization (Milanese et al., 2011; Raiteri et al., 2004). We have recently shown that activation of presynaptic autoreceptors, belonging to mGluR1 and mGluR5 types, by submicromolar concentrations of the mGluR1/5 agonist 3,5-DHPG, promoted an excessive Glu release in the spinal cord of $SOD1^{G93A}$ mice compared to controls (Giribaldi et al., 2013).

Here, we sought to explore whether excessive Group I mGluR activity plays a role in the pathogenesis of ALS. To this end we crossed $SOD1^{G93A}$ mice with mice lacking the mGluR1 ($Grm1^{crv4/+}$; Conti et al., 2006) obtaining double mutants expressing the $SOD1^{G93A}$ mutated gene and half dosage of mGluR1 ($SOD1^{G93A}Grm1^{crv4/+}$).

Materials and methods

Animals

$Grm1^{crv4}$ mice line carrying a recessive loss-of-function mutation (*crv4*) in the gene (*Grm1*) coding for mGluR1 were used to prepare $SOD1^{G93A}Grm1^{crv4/+}$ double mutants. The *crv4* mutation is a spontaneous recessive mutation occurring in the BALB/c/Pas inbred strain. It consists of an insertion of a retrotransposon LTR (Long Terminal Repeat) fragment occurring in intron 4 of the *Grm1* gene and causing the disruption of the gene splicing and the absence of the receptor protein (Conti et al., 2006). Affected ($Grm1^{crv4/crv4}$) and control ($Grm1^{+/+}$) mice were maintained on the same genetic background by intercrossing $Grm1^{crv4/+}$ mice. The genotype of $Grm1^{crv4}$mice was identified by PCR using specific primers as already reported (Conti et al., 2006). B6SJL-Tg(SOD1*G93A)1Gur mice expressing high copy number of mutant human SOD1 with a Gly93Ala substitution ($SOD1^{G93A}$ mice) (Gurney et al., 1994) were originally obtained from Jackson Laboratories (Bar Harbor, ME, USA). Transgenic male mice were crossed with background-matched B6SJL wild-type females and selective breeding maintains the transgene in the hemizygous state. Transgenic mice are identified analyzing tissue extracts from tail tips as previously described (Stifanese et al., 2010). $SOD1^{G93A}$ male mice (on a mixed C57BL6-SJL background) were bred with $Grm1^{crv4/+}$ females (BALB/c background) to generate double-mutants carrying the $Grm1^{crv4/+}$ heterozygous mutation and the SOD1*G93A transgene ($SOD1^{G93A}Grm1^{crv4/+}$). All experiments were conducted on littermates derived from this last breeding (Fig. 1A). Animals were housed at constant temperature (22 ± 1 °C) and relative humidity (50%) with a regular 12 h–12 h light–dark cycle (light 7 AM–7 PM), throughout the experiments. Food (type 4RF21 standard diet obtained from Mucedola, Settimo Milanese, Milan, Italy) and water were freely available. All experiments were carried out in accordance with the European Communities Council Directive of 24 November 1986 (86/609/EEC). All efforts were made to minimize animal suffering and to use only the number of animals necessary to produce reliable results. Sexes were balanced in each experimental group to avoid bias due to sex-related intrinsic differences in disease severity. For experimental use animals were killed at symptomatic stage of disease (19 weeks). A total number of 30 WT, 55 $SOD1^{G93A}$, 55 $SOD1^{G93A}Grm1^{crv4/+}$, and 30 $Grm1^{crv4/+}$ mice were used in this study.

Survival and motor performance

Survival time was identified as the time at which mice were unable to right itself within 20 seconds when placed on their side. The effects of the genetic manipulation on the progression of the disease symptoms were analyzed by Rotarod task and motor deficits. Each clinical test registration was started on day 90 and data were recorded three times a week, until death, in WT, $SOD1^{G93A}$, $SOD1^{G93A}Grm1^{crv4/+}$, and $Grm1^{crv4/+}$ mice. Tests were performed in randomized order by blinded observers. *Rotarod test*: starting on day 90, the time for which an animal could remain on the rotating cylinder was measured using an accelerating Rotarod apparatus (Rota-Rod 7650; Ugo Basile, Comerio, Italy). In this procedure the rod rotation gradually increases in speed from 4 to 40 rpm over the course of 5 min. The time that the mice stayed on the rod until falling off was recorded. Before registration animals were trained for 10 days. *Motor deficits*: mice were rated for disease progression by scoring the extension reflex of hind limbs and the gait. In the extension reflex test, animals were evaluated by observing the hind limb posture when suspended by the tail. Gait deficits were measured by observing mice in an open field. Motor deficits were rated using a 5 point score scale (5, no sign of motor dysfunction; 0, complete impairment) as previously described (Uccelli et al., 2012). *Body weight*: Body weight was measured immediately before behavioral tests. Disease onset was defined retrospectively as the time when mice reached peak of body weight (Boillée et al., 2006b). Animals used in the clinical tests were not used for other experiments.

Histological studies

Tissue preparation

Nineteen-weekold WT, $SOD1^{G93A}$, $SOD1^{G93A}Grm1^{crv4/+}$, and$Grm1^{crv4/+}$ mice were anesthetized with choral hydrate (300 mg/kg) and perfused

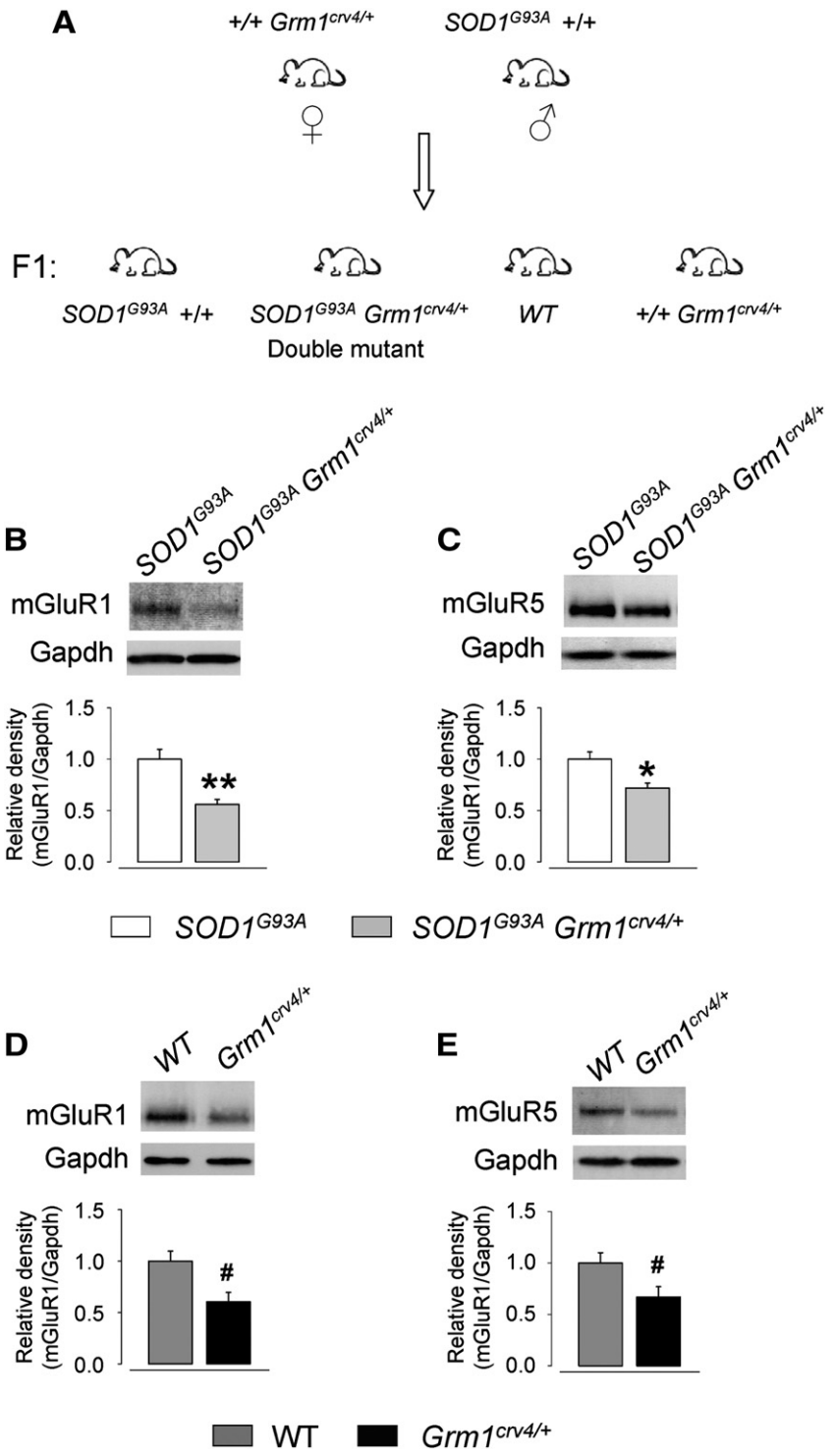

Fig. 1. *Grm1*$^{crv4/+}$and *SOD1*^{G93A}mouse cross and expression of mGluR1 and mGluR5 in spinal cord of WT, *SOD1*^{G93A}, *SOD1*^{G93A}*Grm1*$^{crv4/+}$ and *Grm1*$^{crv4/+}$ mice. Four genetically different mouse littermates (*WT*, *SOD1*^{G93A}, *SOD1*^{G93A}*Grm1*$^{crv4/+}$*Grm1*$^{crv4/+}$) were obtained by crossing Grm1$^{crv4/+}$ and SOD1^{G93A} mice and used for experimental studies (A). Expression of mGluR1 (B and D) and mGluR5 (C and E) in spinal cord lysates was quantified by SDS-PAGE and Western blotting. Mouse anti-mGluR1 monoclonal antibody or rabbit anti-mGluR5 polyclonal antibody was used. mGluR1 and mGluR5 bands were normalized for Gapdh. Representative immunoreactive bands and quantitative analysis (bar plots) are reported. The expression of mGluR1 was halved and that of mGluR5 was reduced by about 30% in both *Grm1*$^{crv4/+}$ and *SOD1*^{G93A}*Grm1*$^{crv4/+}$ mice compared to age-matched WT and *SOD1*^{G93A} animals, respectively. Data are means ± SEM of 7 independent experiments (7 mice per group). *p < 0.05, **p < 0.01 vs. *SOD1*^{G93A}; #p < 0.05 vs. WT (Mann–Whitney).

transcardially with saline followed by 4% paraformaldehyde (PFA) in phosphate buffer (PB, pH 7.4). Spinal cords were post-fixed for 24 h in the same solution at 4 °C and then transferred to a solution containing 30% glycerol, 30% ethylene glycol, 30% distilled water and 10% PB and subsequently stored at −20 °C. Spinal cords were cut coronally into 50-μm-thick sections with a Vibratome; sections were collected into groups of ten. One section/group was stained with 0.1% thionine; subsequently, cervical, thoracic, lumbar and sacral spinal cord levels were identified by light microscopic examination using a Leitz Orthoplan (Wetzlar, Gemany) microscope (Watson et al., 2008). Selected serial lumbar spinal cord levels (L4/L5) were post-fixed in 1% osmium tetroxide in PB for 45 min, and contrasted with 1% uranyl acetate in maleate

buffer (pH 6.0; 1 h). After dehydration in ethanol and propylene oxide, sections were embedded in Epon/Spurr resin (Electron Microscopy Sciences, Hatfield, PA, USA), flattened between Aclar sheets (Electron Microscopy Sciences) and polymerized at 60 °C for (48 h). Small blocks of tissue containing ventral horn and ventrolateral funiculus (Jaarsma et al., 2000) were selected by light-microscopic inspection, glued to blank epoxy and sectioned with an ultra-microtome (MTX; Research and Manufacturing Company Inc., Tucson, AZ, USA). Ultrathin sections (60 nm) were collected and mounted on 200 mesh copper grids, stained with uranyl acetate and Sato's lead and examined with a Philips EM 208 electron microscope coupled to a MegaViewII high-resolution CCD camera (Soft Imaging System; Munster, Germany).

Data analysis

For light microscopy studies, number of 0.1% thionine positive alpha-motoneurons in ventrolateral horn of L4/L5 was estimated using serial 50 μm sections from WT (17 sections/2 animals), *SOD1*^{G93A} mutant (14 sections/3 animals), *SOD1*^{G93A}*Grm1*$^{crv4/+}$double mutant (14 sections/3 animals) and *Grm1*$^{crv4/+}$ mice (15 sections/2 animals). Microscopic fields of ventrolateral horns were captured with a digital camera coupled to Leitz Orthoplan microscope; alpha-motoneurons were selected and counted based on diameters greater than 25 μm using ImageJ version 1.29 software (NIH, Bethesda, MD, USA). For electron microscopy analysis, the morphology of both normal and abnormal mitochondria in neuronal perikarya, dendrites, myelinated axons and axon terminals of selected motoneurons was studied. For each experimental group (10–12 ultrathin sections/animal; 3 animals) quantitative data on normal and swollen/vacuolated mitochondria were gathered from the analysis of at least 40 microscopic fields/compartment, corresponding to a total area of about 800 μm^{2}for each experimental condition. Microscopic fields were randomly selected and captured at 18,000 or 22,000×. To determine the relative density of normal and swollen/vacuolated mitochondria, areas of each cellular compartment were calculated using ImageJ version 1.29 software (NIH, Bethesda, MD, USA); normal and abnormal mitochondria were identified and counted as previously described (Jaarsma et al., 2000; Sasaki et al., 2004).

Quantification of protein expression

Spinal cord from 19-week old WT, *SOD1*^{G93A}, *SOD1*^{G93A}*Grm1*$^{crv4/+}$, and *Grm1*$^{crv4/+}$mice were dissected and homogenized in lysis buffer (10 mM Tris, pH 8.8, 20% glycerol, 2% sodium dodecyl sulfate, 0.1 mM EDTA, 5% β-mercaptoethanol). Protein concentration was determined according to Bradford (1976). Appropriate amount of total protein was separated by means of SDS-polyacrylamide gel electrophoresis. The concentration of proteins in each sample felt in the linear portion of the curve. A triplicate analysis for each sample was performed. Electroblotted proteins were monitored using Naphthol blue black staining (Sigma-Aldrich, St Louis, MO, USA). Membranes were then incubated with the following antibodies: anti-Glial Fibrillar Acidic Protein (GFAP) mouse monoclonal antibody (1:5000; Sigma Aldrich, St Louis, MO, USA); anti-ionizing calcium-binding adaptor molecule 1 (IBA-1) goat polyclonal antibody (1:1000; Abcam, Cambridge, UK); anti-mGluR1 mouse monoclonal antibody (1:2500; BD Biosciences, San Jose, CA, USA); anti-mGluR5 rabbit polyclonal antibody (1:10000, Epitomics, Burlingame, CA, USA); anti-GLT1 mouse monoclonal antibody (1:5000), and anti-Gapdh mouse monoclonal antibody (1:10000; Millipore, Billerica, MA, USA). After incubation with appropriate peroxidase-coupled secondary antibodies, protein bands were detected by using a Western blotting detection system (ECL Advance™; Amersham Biosciences, Piscataway, NJ, USA). Bands were detected and analyzed for density using an enhanced chemiluminescence system (Versa-Doc 4000; Bio-Rad, Segrate, Milan, Italy), and Quantity One software (Bio-Rad). Bands of interest were normalized for Gapdh level in the same membrane.

Quantification of gene expression

Spinal cord from 19-week old WT, *SOD1*^{G93A}, *Grm1*$^{crv4/+}$, *SOD1*^{G93A}*Grm1*$^{crv4/+}$mice were dissected, quickly frozen in liquid nitrogen and stored at −80 °C until use. Total RNA was isolated by means of the acid phenol-chloroform procedure, using the Trizol reagent (Sigma Aldrich, St Louis, MO, USA) according to the manufacturers' instructions, converted to cDNA and amplified with the Chromo 4^{TM} System real-time PCR apparatus (Biorad, Milan, Italy, 17). Analysis of the expression levels of metallothionein 1, 2, 3 (MT-1, MT-2, MT-3) and catalase genes was carried out as previously described (Lanza et al., 2009). Real-time PCR reactions were performed in a final volume of 20 μL containing 10 ng cDNA, 10 μL of iTaq SYBR Green Supermix with ROX (Bio-Rad), and 0.25 μM of each primer pair (TIB MolBiol, Genoa, Italy). Glyceraldehyde 3-phosphate dehydrogenase (Gapdh) was used as reference gene. The mRNA expression levels of MTs and catalase of each experimental group of mice were normalized to Gapdh and represented as relative to the WT mice (normalized fold change).

Release experiments

WT, *SOD1*^{G93A}, *SOD1*^{G93A}*Grm1*$^{crv4/+}$, and *Grm1*$^{crv4/+}$ 19-week old mice were sacrificed, the spinal cord rapidly dissected and synaptosomes prepared and purified as previously described (Giribaldi et al., 2013). Synaptosomes were resuspended in physiological medium and labeled with 0.05 μM [^{3}H]D-Asp, used as a tracer of the intraterminal pools of Glu (Fleck et al., 2001). Aliquots were distributed on microporous filters placed at the bottom of a set of parallel superfusion chambers maintained at 37 °C (Superfusion System, Ugo Basile, Comerio, Varese, Italy; Raiteri et al., 1984) and the effect of (S)-3,5-Dihydroxyphenylglycine (3,5-DHPG; 0.3 and 30 μM) on [^{3}H]D-Asp release was studied. Superfusion was started with physiological medium at a rate of 0.5 ml/min and continued for 48 min. After 36 min of superfusion to equilibrate the system, five 3-min samples were collected. (S)-3,5-Dihydroxyphenylglycine (3,5-DHPG; 0.3 and 30 μM) was introduced at the end of the first sample collected (t = 39 min) and maintained until the end of the experiment. Collected samples and superfused synaptosomes were counted for radioactivity. Tritium released in each sample was calculated as fractional rate × 100 (percentage of the total synaptosomal neurotransmitter content at the beginning of the respective collection period). Drug effects were evaluated by calculating the ratio between the efflux in the fourth sample collected (in which the maximum effect of 3,5-DHPG was generally reached) and the efflux of the first fraction (basal efflux). This ratio was compared to the corresponding ratio obtained under resting conditions. Appropriate controls were always run in parallel.

Statistics

Data are expressed as mean ± SEM and p value <0.05 was considered significant. The Kaplan–Meier plot was used to evaluate survival probability and cumulative curves were compared using the log-rank test. The Mann Whitney test was used to compare two mean populations. Multiple comparisons were performed using the analysis of variance (ANOVA) followed by Bonferroni or Barlett post hoc test. Analyses were performed by means of Graph Prism (GraphPad Software, Inc., San Diego, CA, USA) and SigmaStat (Systat Software, Inc., San Jose, CA, USA) softwares.

Results

Generation of SOD1^{G93A} *Grm1*$^{crv4/+}$ *mice*

To obtain mice expressing the human G93A-mutated SOD1 and half dosage of mGluR1, we crossed *SOD1*^{G93A} transgenic mice with the

Grm1$^{crv4/+}$ mouse line carrying a recessive loss-of-function mutation (*crv4*) in the gene (*Grm1*) coding for mGluR1, thus obtaining four different genotypes (Fig. 1A). *Grm1*$^{crv4/crv4}$ homozygous mice present substantial motor coordination deficits, while heterozygous *Grm1*$^{crv4/+}$ do not exhibit anomalous neurological phenotype. Heterozygous *Grm1*$^{crv4/+}$ mice carrying the *SOD1*^{G93A} transgene (*SOD1*^{G93A}Grm1$^{crv4/+}$ double mutants) from the initial crossing were then crossed with *Grm1*$^{crv4/+}$ animals. All genotypes were born at the expected Mendelian ratio and were indistinguishable from wild-type littermates at birth, with the exception of *Grm1*$^{crv4/crv4}$ mice that showed impaired coordination of hind limbs, reduced size and shorter life span, particularly evident in the double mutants *SOD1*^{G934}*Grm1*$^{crv4/crv4}$. To answer the question whether the reduced expression of mGluR1 improved the phenotype of *SOD1*^{G93A} mice, we focused on mice carrying only one functional allele of mGluR1, *SOD1*^{G93A}Grm1$^{crv4/+}$, and we no longer considered the *SOD1*^{G93A}*Grm1*$^{crv4/crv4}$ mice, thus avoiding to add the deleterious neurological effects due to the complete absence of mGluR1 to the *SOD1*^{G93A} neurological phenotype.

Spinal cord lysates of *SOD1*^{G93A} and *SOD1*^{G93A}*Grm1*$^{crv4/+}$ mice were analyzed for mGluR1 (Fig. 1B) or mGluR5 (Fig. 1C) expression. The results obtained highlighted that mGluR1 expression was halved in *SOD1*^{G93A}Grm1$^{crv4/+}$ compared to *SOD1*^{G93A} mice. Interestingly, also mGluR5 expression was reduced by almost 30%,when comparing the same mouse groups. As expected, mGluR1 was halved in *Grm1*$^{crv4/+}$ respect to WT mice (Fig. 1D). A similar reduction was observed when studying the expression of mGluR5 in *Grm1*$^{crv4/+}$ vs. WT mice (Fig. 1E).

Survival and motor functions are improved in SOD1^{G93A}*Grm1*$^{crv4/+}$*mice*

Decreasing mGluR1 expression significantly prolonged the life span of *SOD1*^{G93A}*Grm1*$^{crv4/+}$ double mutants compared to *SOD1*^{G93A} mice. The Kaplan–Meier survival probability curve is reported in Fig. 2A.

Starting around day 115 of life, *SOD1*^{G93A} mice showed a significant decrease of body weight compared to WT mice (Fig. 2B). The decrease of body weight became significant only around day 140 in *SOD1*^{G93A}*Grm1*$^{crv4/+}$mice. Weight decrease was always less pronounced

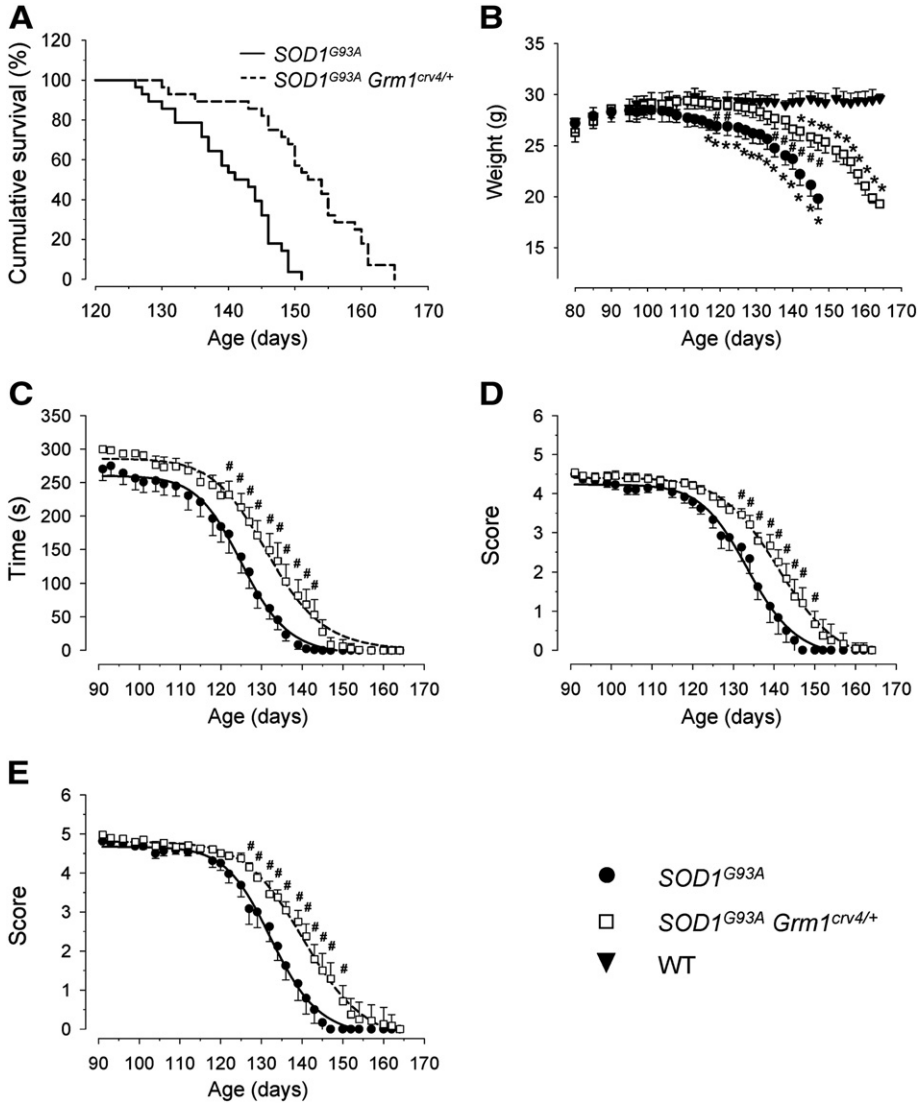

Fig. 2. Survival and disease progression in *SOD1*^{G93A} and *SOD1*^{G93A}*Grm1*$^{crv4/+}$ mice. Survival time was assumed as the time when animals were unable to right itself within 20 seconds when placed on their side. Twenty-eight mice per group were used. Kaplan–Meyer analysis was used to determine survival probability (A). The difference between Kaplan–Meyer curves was significant at $p < 0.001$ (Log-rank test). Body weight (B) was measured immediately before behavioral tests. The body weight of WT mice was also measured to determine the related peak of body weight in pathological animals as hallmark of disease onset. Rotarod (C), hind limbs extension reflex (D) and gait impairment (E) were analyzed to determine the disease progression. Animals were tested 3 days a week starting on day 90. Falling off time was recorded in Rotarod experiments. Animals were rated according to a 5–0 score scale in hind limb extension and gait impairment observations (Uccelli et al., 2012). Survival probability and behavioral abilities were significantly augmented in *SOD1*^{G93A}*Grm1*$^{crv4/+}$ compared to *SOD1*^{G93A} mice, indicating a slower disease progression. The decrease of body weight took place later in *SOD1*^{G93A}*Grm1*$^{crv4/+}$ compared to *SOD1*^{G93A} mice, indicating a delay in the disease onset. Data reported in B–E are means ± SEM of 12 mice per group; $^{*}p < 0.05$ at least vs. WT; $^{\#}p < 0.05$ at least vs. *SOD1*^{G93A} (Mann–Whitney Rank Sum Test).

in *SOD1*^{G93A}*Grm1*$^{crv4/+}$ than in *SOD1*^{G93A} mice. The difference in the start of weight loss between *SOD1*^{G93A}*Grm1*$^{crv4/+}$ and *SOD1*^{G93A} suggests that halving the dosage of mGluR1 in *SOD1*^{G93A} mice delays the disease onset (Boillée et al., 2006b).

To verify whether the reduction of mGluR1 expression slowed disease progression, we subjected *SOD1*^{G93A} and *SOD1*^{G93A}*Grm1*$^{crv4/+}$ mice to a number of behavioral tests, such as Rotarod, posterior limb extension reflex, gait impairment. As expected, the performance of *SOD1*^{G93A} mice in Rotarod (Fig. 2C), extension reflex (Fig. 2D) and gait impairment (Fig. 2E) tasks were superimposable to that of control healthy mice (not shown in the figure) until around day 80, then it rapidly worsened. Interestingly, *SOD1*^{G93A}*Grm1*$^{crv4/+}$ mice performed significantly better than *SOD1*^{G93A} mice in all tasks (Figs. 2C–E). All together, behavioral tests suggest that halving the dosage of mGluR1 in *SOD1*^{G93A} mice results in a remarkable slowing down of the neurological ALS phenotype progression.

Motoneurons are preserved in SOD1^{G93A}*Grm1*$^{crv4/+}$ *mice*

Since one of the main features of ALS is the progressive loss of spinal MNs (Shaw and Eggett, 2000), we assessed their number by light microscopic inspection of ventral horns in lumbar spinal cord sections (L4/L5) of WT, *SOD1*^{G93A}, *SOD1*^{G93A}*Grm1*$^{crv4/+}$ and *Grm1*$^{crv4/+}$ mice. This analysis revealed comparable gross histological features in WT and *Grm1*$^{crv4/+}$ mice, low tissue preservation associated with severe neuronal loss in *SOD1*^{G93A} mice, and intermixable histological features in *SOD1*^{G93A}*Grm1*$^{crv4/+}$ mice (Fig. 3, left). The number of MNs was significantly increased in *SOD1*^{G93A}*Grm1*$^{crv4/+}$ double mutant mice, compared to *SOD1*^{G93A} mice (Fig. 3, right). MN number was 28.6 ± 1.0, 4.8 ± 0.4, 11.8 ± 0.5 and 27.7 ± 1.5 in WT, *SOD1*^{G93A}, *SOD1*^{G93A}*Grm1*$^{crv4/+}$, and *Grm1*$^{crv4/+}$mice, respectively. These findings indicate that halving the dosage of mGluR1 in *SOD1*^{G93A} mice preserves MNs from death.

Astrogliosis and microgliosis are reduced in SOD1^{G93A}*Grm1*$^{crv4/+}$ *mice*

Astrocyte activation and microgliosis are key features of ALS (Lasiene and Yamanaka, 2011; Rossi et al., 2008). We investigated the expression of GFAP and IBA-1, as markers for reactive astrocytes and microglia, respectively, in WT, *SOD1*^{G93A}, *SOD1*^{G93A} *Grm1*$^{crv4/+}$and *Grm1*$^{crv4/+}$ mice. The expression of GFAP was significantly higher in *SOD1*^{G93A} mice compared to WT and *Grm1*$^{crv4/+}$ control mice and GFAP over-expression was reversed in *SOD1*^{G93A}*Grm1*$^{crv4/+}$mice (Fig. 4A). Similarly, the expression of IBA-1 was higher in *SOD1*^{G93A} mice compared to WT and *Grm1*$^{crv4/+}$ mice and it was reduced back to control levels in *SOD1*^{G93A}*Grm1*$^{crv4/+}$ mice (Fig. 4B). The above results suggest that halving the dosage of mGluR1 in *SOD*^{G93A} background produces normalization of astrocyte and microglia activation.

The reduction of GLT1 expression is not rescued in SOD1^{G93A}*Grm1*$^{crv4/+}$ *mice*

GLT1 expression is reduced in animal models of ALS and in patients (Dunlop et al., 2003; Howland et al., 2002; Rothstein et al., 1995). We measured the expression of the glutamate transporters in the spinal cord of WT, *SOD1*^{G93A}, *SOD1*^{G93A} *Grm1*$^{crv4/+}$and *Grm1*$^{crv4/+}$ mice. As expected, the expression of GLT1 was significantly lower (about 40%) in *SOD1*^{G93A} mice vs. WT mice and also when compared to *Grm1*$^{crv4/+}$ mice. GLT1 expression was not modified in *SOD1*^{G93A}*Grm1*$^{crv4/+}$ respect to *SOD1*^{G93A} mice (Fig. 5). These results suggest that halving the dosage of mGluR1 in *SOD*^{G93A} background does not interfere with GLT1 expression.

Metallothionein mRNA expression and catalase are normalized in SOD1^{G93A}*Grm1*$^{crv4/+}$ *mice*

It is known that the G93A mutation in SOD1 leads to oxidative stress (Robberecht, 2000). We monitored the mRNA expression of MT1, MT2 and MT3, as markers for oxidative stress in the spinal cord of WT, *SOD1*^{G93A}, *SOD1*^{G93A}*Grm1*$^{crv4/+}$ and *Grm1*$^{crv4/+}$ mice (Gong and Elliott, 2000; Uccelli et al., 2012). The mRNA coding for all MTs was significantly increased in the spinal cord of *SOD1*^{G93A} compared to both WT and *Grm1*$^{crv4/+}$ control mice (Figs. 6A,B,C). MT mRNA expression did not change significantly between *Grm1*$^{crv4/+}$ and WT mice. Of note, *SOD1*^{G93A}*Grm1*$^{crv4/+}$ mice displayed a down-regulation of the MT mRNA expression and this reduction was significant for MT1 and MT3 (Figs. 6A and C).

It has been reported that an impairment of catalase (CAT) activity in both sporadic ALS and familial ALS patients is an index of impaired antioxidant mechanisms (Babu et al., 2008; Nikolić-Kokić et al., 2006). Interestingly, we found a significant decrease of CAT mRNA expression in *SOD1*^{G93A} respect to WT mice and this reduction was reverted in *SOD1*^{G93A}*Grm1*$^{crv4/+}$ (Fig. 6D). No differences were measured between Grm1$^{crv4/+}$ and WT mice. These data suggest that halving the dosage of mGluR1 in *SOD*^{G93A} background produced normalization of MTs and CAT mRNA expression.

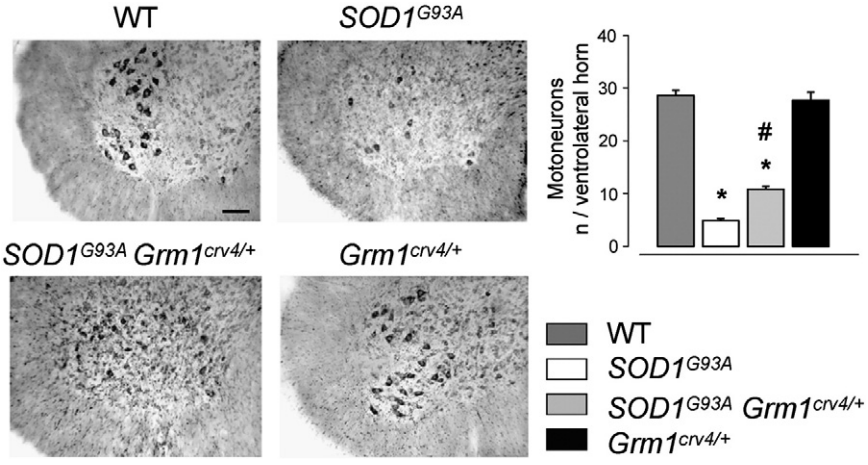

Fig. 3. Number of motoneurons in spinal cord from WT, *SOD1*^{G93A}, *SOD1*^{G93A}*Grm1*$^{crv4/+}$ and *Grm1*$^{crv4/+}$ mice. Mice were anesthetized and perfused transcardially with paraformaldehyde. Spinal cords were post-fixed and stored at −20 °C. Lumbar (L4/L5) sections (50 μm-thick) were stained with thionine. Alpha-motoneurons were selected and counted based on diameters greater than 25 μm. Representative photomicrographs of lumbar spinal cord sections (left; scale bar 100 μm) and quantitative analysis (right) are reported. The dramatic loss of motoneurons observed in *SOD1*^{G93A} mice was significantly reduced in *SOD1*^{G93A}*Grm1*$^{crv4/+}$ mice. Data are means ± SEM of 15 sections, at least, from 3 mice per group.*$p < 0.01$ vs. WT; #$p < 0.01$ vs. *SOD1*^{G93A} (one-way ANOVA and Bartlett's post-hoc tests).

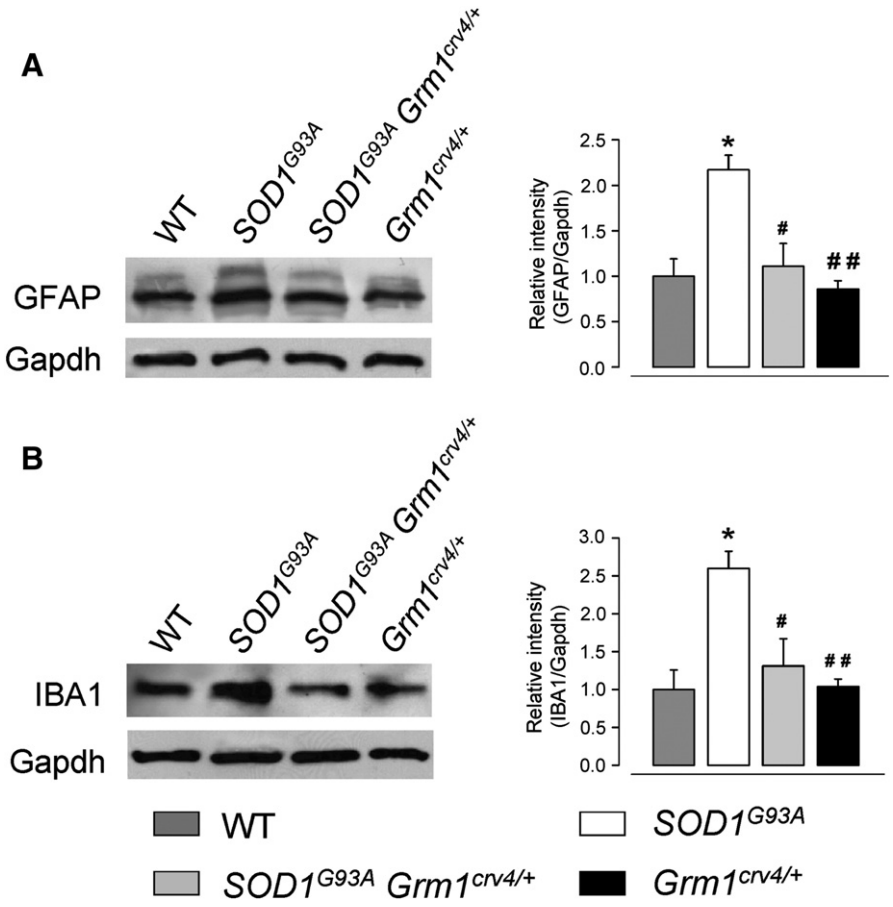

Fig. 4. Astrogliosis and microgliosis in spinal cord from WT, *SOD1*^{G93A}, *SOD1*^{G93A}*Grm1*$^{crv4/+}$ and *Grm1*$^{crv4/+}$mice. The expression of GFAP (A) and IBA-1 (B) was measured as an index of astrogliosis and activated microglia, respectively. GFAP and IBA-1 were determined in lumbar spinal cord homogenates by SDS-PAGE and Western blotting using a mouse anti-GFAP monoclonal antibody or a goat anti-IBA-1 polyclonal antibody. Representative immunoreactive bands (left panels) and quantitative analysis (right panels) are reported. Over-expression of both GFAP and IBA-1 detected in *SOD1*^{G93A} mice was almost normalized in *SOD1*^{G93A}*Grm1*$^{crv4/+}$ mice. Data are means ± SEM of 6 independent experiments (6 mice per group).*$p < 0.005$ vs. WT; $^{\#}p < 0.01$, $^{\#\#}p < 0.005$ vs. *SOD1*^{G93A} (one-way ANOVA and Bonferroni's post-hoc tests).

Mitochondrial damage is reduced in SOD1^{G93A}*Grm1*$^{crv4/+}$ *mice*

Electron microscopy analysis of perikarya, dendrites, myelinated axons and axon terminals of motoneurons was performed to quantify the degree of mitochondrial abnormalities, a sensitive index of neurodegenerative progression (Cozzolino and Carrì, 2012). Fig. 7A illustrates representative electron micrographs obtained in L4/L5 spinal cord sections from WT, *SOD1*^{G93A}, *SOD1*^{G93A}*Grm1*$^{crv4/+}$ and *Grm1*$^{crv4/+}$ mice. As shown in Fig. 7B, the density of normal mitochondria was significantly lower and that of swollen/vacuolated mitochondria

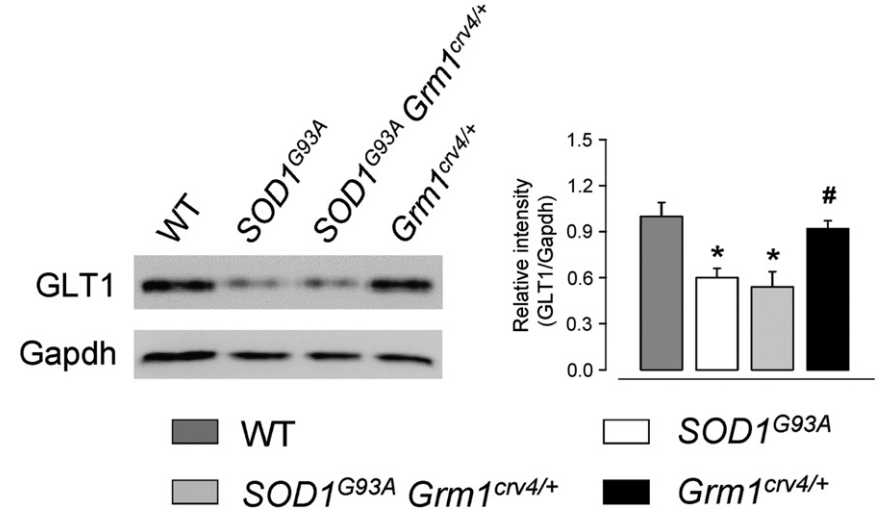

Fig. 5. Glutamate transporter 1 expression in spinal cord from WT, *SOD1*^{G93A}, *SOD1*^{G93A}*Grm1*$^{crv4/+}$ and *Grm1*$^{crv4/+}$mice. The expression of GLT1 was measured in lumbar spinal cord homogenates by SDS-PAGE and Western blotting using a mouse anti-GLT1 monoclonal antibody. Representative immunoreactive bands (left panels) and quantitative analysis (right panels) are reported. The expression of GLT1 was reduced in *SOD1*^{G93A} and *SOD1*^{G93A}*Grm1*$^{crv4/+}$ mice with respect to WT or *Grm1*$^{crv4/+}$ mice. Data are means ± SEM of 4 independent experiments (4 mice per group).*$p < 0.05$ vs. WT; $^{\#}p < 0.05$ vs. *SOD1*^{G93A} (one-way ANOVA and Bonferroni's post-hoc tests).

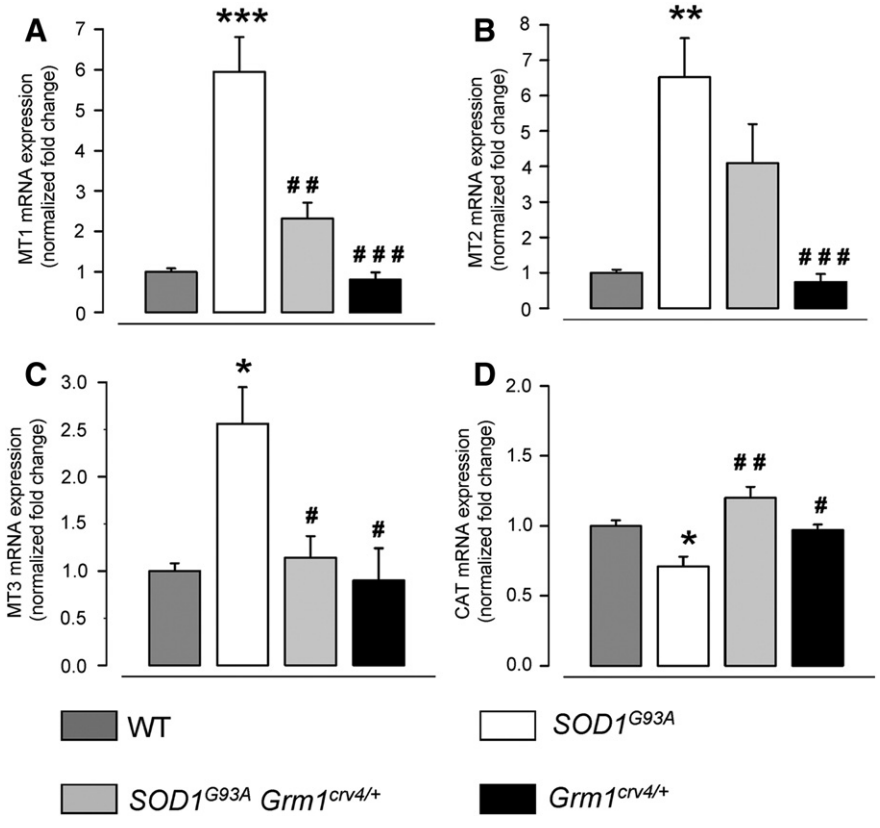

Fig. 6. Metallothionein and catalase mRNA expression in spinal cord from WT, *SOD1^{G93A}*, *SOD1^{G93A}Grm1$^{crv4/+}$* and *Grm1$^{crv4/+}$*mice. The expression of metallothioneins (MT1 panel A, MT2 panel B and MT3 panel C) and catalase (CAT, panel D) were detected in lumbar spinal cord extracts by RT-PCR. Gapdh was used as reference gene. Gene expression is reported as relative mRNA amount (normalized fold change) compared to WT mice. Over-expression of MTs mRNA and CAT mRNA down regulation detected in *SOD1^{G93A}* mice are normalized in *SOD1^{G93A}Grm1$^{crv4/+}$*mice. Data are means ± SEM of 5 independent experiments (5 mice per group; 2 mRNA extractions for each mouse). $^{*}p < 0.05$, $^{**}p < 0.01$, $^{***}p < 0.001$ vs. WT; $^{\#}p < 0.05$, $^{\#\#}p < 0.005$,$^{\#\#\#}p < 0.001$ vs. *SOD1^{G93A}* (one-way ANOVA and Bonferroni post-hoc tests).

significantly higher in perikarya of *SOD1^{G93A}* compared to WT mice. Accordingly, the number of swollen/vacuolated mitochondria was significantly lower in *SOD1^{G93A}Grm1$^{crv4/+}$* and *Grm1$^{crv4/+}$* compared with *SOD1^{G93A}* mice and it was not significantly different comparing *SOD1^{G93A}Grm1$^{crv4/+}$* to WT or *Grm1$^{crv4/+}$*mice. In dendrites, the density of normal mitochondria differed between WT and *SOD1^{G93A}* and between *SOD1^{G93A}* and *Grm1$^{crv4/+}$*mice, but not between *SOD1^{G93A}* and *SOD1^{G93A}Grm1$^{crv4/+}$*. The number of swollen/vacuolated mitochondria was significantly higher in *SOD1^{G93A}* when compared to the other experimental groups, which did not differ significantly. In axons, the density of normal mitochondria differed in WT compared to *SOD1^{G93A}* and in *SOD1^{G93A}* compared to *Grm1$^{crv4/+}$* mice, but not between *SOD1^{G93A}* and *SOD1^{G93A}Grm1$^{crv4/+}$* mice, in spite of the robust difference observed. A significant difference was also found between WT and *SOD1^{G93A}Grm1$^{crv4/+}$*mouse normal mitochondria. The density of swollen/vacuolated mitochondria in axons was significantly different only between WT and *SOD1^{G93A}* groups. As far as the number of the normal mitochondria in axon terminals is concerned, significant differences were observed between *SOD1^{G93A}* and WT, *SOD1^{G93A}Grm1$^{crv4/+}$* and *SOD1^{G93A}*, and between *Grm1$^{crv4/+}$* and *SOD1^{G93A}Grm1$^{crv4/+}$*, *Grm1$^{crv4/+}$* and WT groups. The density of swollen/vacuolated mitochondria in axon terminals was significantly different only when WT and *SOD1^{G93A}* mice were compared.

Summarizing the data described in Fig. 7, both perikarya and dendrites displayed a reduction of swollen/vacuolated mitochondria and an increase of normal mitochondria in *SOD1^{G93A}Grm1$^{crv4/+}$* compared to *SOD1^{G93A}* mice. Axons of *SOD1^{G93A}Grm1$^{crv4/+}$* mice showed a small non-significant increase of normal mitochondria and a small non-significant decrease of swollen/vacuolated mitochondria compared to *SOD1^{G93A}* mice. Axon terminals of *SOD1^{G93A}Grm1$^{crv4/+}$* mice showed an increase of normal mitochondria density compared to *SOD1^{G93A}* and a decrease, though not significant, of swollen/vacuolated mitochondria. Thus, halving the dosage of mGluR1 in *SOD1^{G93A}* background results in the histological amelioration of mitochondria characteristics.

Excessive [^{3}H]D-aspartate release is normalized in SOD1^{G93A}Grm1$^{crv4/+}$ mice

Our previous study demonstrated an excessive Glu release evoked by mGluR1 and mGluR5 activation in synaptosomes purified from lumbar spinal cord of *SOD1^{G93A}* mice (Giribaldi et al., 2013). To assess whether dampening mGluR1 expression, leading also to reduction of the expression of mGluR5, could modify this abnormal effect, we performed experiments comparing the release of [^{3}H]D-Asp induced by the mGluR1/5 agonist 3,5-DHPG in WT, *SOD1^{G93A}*, *SOD1^{G93A}Grm1$^{crv4/+}$*and *Grm1$^{crv4/+}$* mice. Fig. 8 shows that [^{3}H]D-Asp release evoked by 0.3 μM 3,5-DHPG was increased in *SOD1^{G93A}* with respect to WT mice. Of note, the 3,5-DHPG-evoked release was reduced to control levels in *SOD1^{G93A}Grm1$^{crv4/+}$* mice. No differences were observed in comparing WT, *SOD1^{G93A}Grm1$^{crv4/+}$* and *Grm1$^{crv4/+}$*mice. Also the 30 μM 3,5-DHPG-evoked release of [^{3}H]D-Asp was increased in *SOD1^{G93A}* mice. [^{3}H]D-Asp release was even significantly lower in *SOD1^{G93A}Grm1$^{crv4/+}$*and *Grm1$^{crv4/+}$* mice when compared to WT mice. Thus, halving the dosage of mGluR1 in*SOD^{G93A}* background normalizes the excessive Group I mGluR-induced [^{3}H]D-Asp release.

Discussion

Glu-mediated excitotoxicity is one of the major determinants of ALS. In a previous work we have demonstrated that abnormal release of excitatory amino acid neurotransmitters occurs at the spinal cord level in the *SOD1^{G93A}* mouse model of human ALS (Giribaldi et al., 2013;

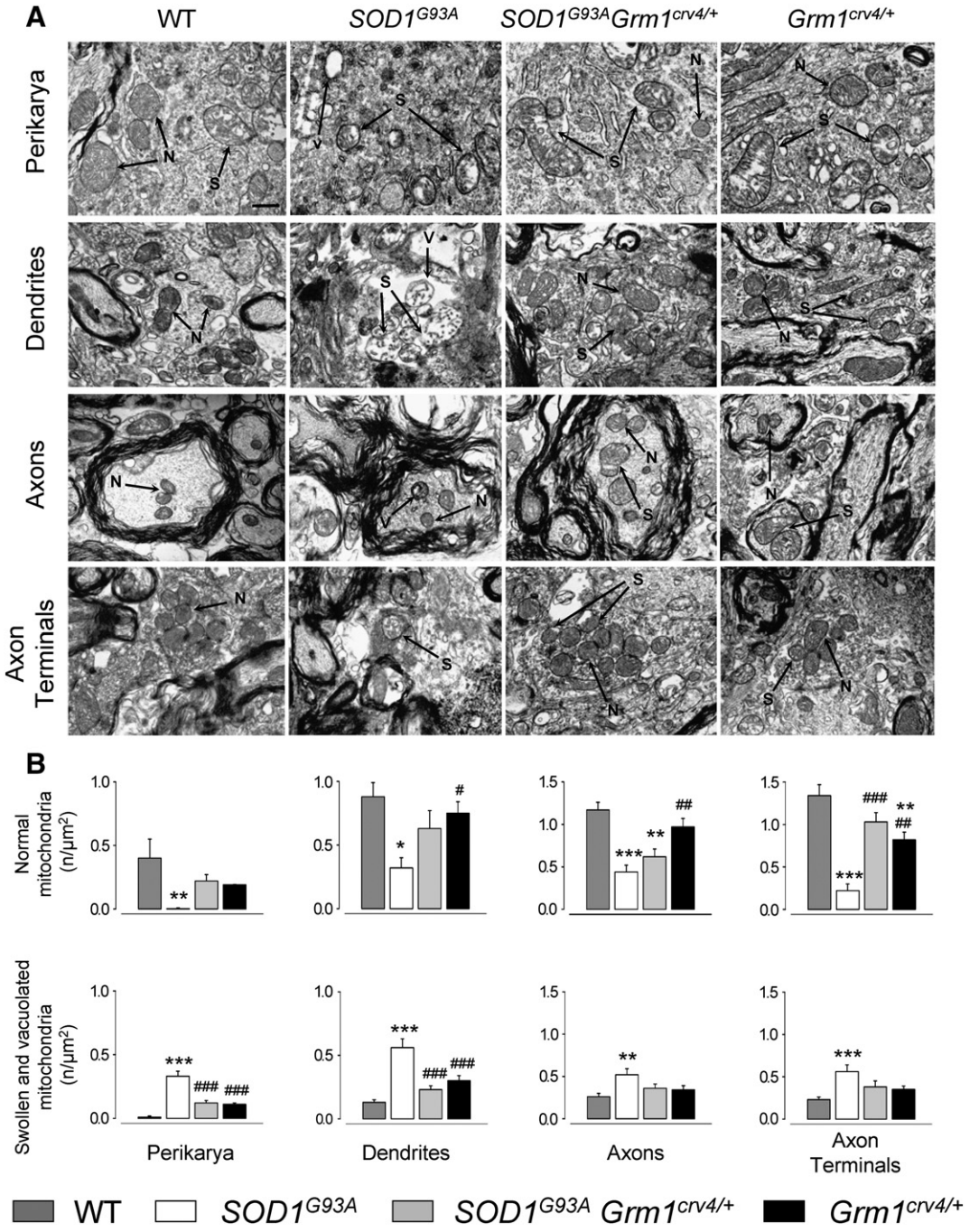

Fig. 7. Electron microscopy analysis of mitochondria in spinal cord from WT, *SOD1*^{G93A}, *SOD1*^{G93A}*Grm1*$^{crv4/+}$and *Grm1*$^{crv4/+}$mice. Ultrathin sections (60 nm) from lumbar (L4/L5) spinal cord were stained with uranyl acetate and Sato's lead and examined by EM coupled to a high-resolution CCD camera. Normal and swollen/vacuolated mitochondria were quantified in perikarya, dendrites, myelinated axons and axon terminals in motoneurons. Representative photomicrographs (A; scale bar: 1 μm) and quantitative analysis (B) are reported. Black arrows indicate normal (N) and swollen (S) or vacuolated (V) mitochondria. Data are expressed as number/μm of normal and swollen/vacuolated mitochondria and are means ± SEM of 40 microscopic fields, at least, from 3 mice per group, corresponding to a total area of about 800 μm^2. Normal mitochondria were dramatically reduced and swollen/vacuolated mitochondria increased in *SOD1*^{G93A} mice. In *SOD1*^{G93A}*Grm1*$^{crv4/+}$, normal mitochondria were significantly augmented in perikarya, dendrites and axon terminals and swollen/vacuolated mitochondria were significantly reduced in perikarya and dendrites. $^{*}p < 0.05$, $^{**}p < 0.01$, $^{***}p < 0.001$ vs. WT; $^{\#}p < 0.05$, $^{\#\#}p < 0.01$, $^{\#\#\#}p < 0.001$ vs. *SOD1*^{G93A} (one-way ANOVA and Bartlett's post-hoc tests).

Milanese et al., 2010, 2011; Raiteri et al., 2003, 2004). During these studies, it emerged that mGluR1 and mGluR5 could play a role in the process. Indeed, exposure to the mGluR1/5 agonist 3,5-DHPG at concentrations >0.3 μM stimulated Glu release in the lumbar spinal cord of both control and *SOD1*^{G93A} mice. At variance, concentrations of 3,5-DHPG ≤0.3 μM increased Glu release in *SOD1*^{G93A} mice only. The use of selective antagonists and of confocal and electron microscopy experiments indicated the involvement of presynaptically located mGluR1 and mGluR5, mGluR5 being preferentially involved in the high potency effects of 3,5-DHPG (Giribaldi et al., 2013). Therefore, activation of mGluR1 and mGluR5 produces abnormal glutamate release in *SOD1*^{G93A} mice, suggesting that these receptors are implicated in ALS. In order to support this hypothesis, we studied here the impact of mGluR1 in the progress of experimental ALS by down-regulating mGluR1 expression in the *SOD1*^{G93A} genetic background. The results obtained indicate that reducing mGluR1 ameliorates the course of the disease, attaining a significant increase of life span as well as a delay in the disease onset and progression and ameliorates a number of histological

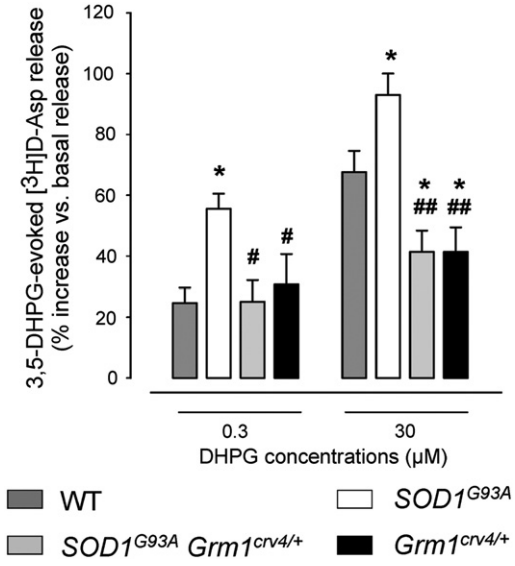

Fig. 8. Glutamate release evoked by 3,5-DHPG in spinal cord from WT, $SOD1^{G93A}$, $SOD1^{G93A}Grm1^{crv4/+}$ and $Grm1^{crv4/+}$ mice. Spinal cord synaptosomes were labeled with [^{3}H]D-Asp and exposed in superfusion to 0.3 and 30 μM of 3,5-DHPG. Superfusion samples were counted for radioactivity. Results are expressed as per cent increase of basal release. The abnormal 3,5-DHPG-evoked [^{3}H]D-Asp release detected in $SOD1^{G93A}$ mice was abolished in $SOD1^{G93A}Grm1^{crv4/+}$ mice. Data are means ± SEM of 8–10 independent experiments (8–10 mice per group) run in triplicate.*$p < 0.05$ vs. WT; $^{\#}p < 0.05$, $^{\#\#}p < 0.001$ vs. $SOD1^{G93A}$ (one-way ANOVA and Bonferroni post-hoc tests).

and biochemical readouts which are profoundly altered in $SOD1^{G93A}$ mice.

Noteworthy, halving mGluR1 expression also leads to a reduction of mGluR5 in $SOD1^{G93A}Grm1^{crv4/+}$mouse spinal cord. On this basis, it could be hypothesized that the presence of the genetic *cerv4* mutation in the $SOD1^{G93A}$ background can reduce mGluR5 expression by an unknown homeostatic mechanism, possibly linked to the molecular and functional interplay existing between the two Group I mGlu receptors (Fazio et al., 2008; Rossi et al., 2012). Of note, also $Grm1^{crv4/+}$ mice show lower levels of mGluR5 compared to WT mice. Whichever the reason, the lower levels of mGluR5 found in $SOD1^{G93A}Grm1^{crv4/+}$ mice suggest that both Group I mGluR subtypes play a role in the functional and biochemical changes observed. Further studies are in progress to clarify the effects of mGluR5 dampening in the $SOD1^{G93A}$ mouse model of ALS.

A typical hallmark of ALS end stage is the massive loss of spinal cord MNs. We showed here that halving mGluR1 in the $SOD1^{G93A}$ background significantly increases the number of MNs still present in the ventral horns of the affected lumbar spinal cord. This preservation may be at the basis of the amelioration and, possibly, of the delayed onset of symptoms above reported. Further studies aimed at monitoring the loss of MNs in $SOD1^{G93A}Grm1^{crv4/+}$ respect to $SOD1^{G93A}$ mice during disease progression would help to strengthen this correlation.

MN damage in ALS is a non-cell autonomous event and this occurrence adds complexity to ALS etiology. Although neuron-restricted mutated SOD1 expression is sufficient to cause MN death, mutated SOD1 expression in surrounding astrocytes and microglia influences the progression rate of neurodegeneration (Ilieva et al., 2009; Li et al., 2011). In this scenario, astrocytes promise to play a pivotal role by affecting disease progression (Wang et al., 2011b; Yamanaka et al., 2008) and MN vulnerability to excitotoxicity (Van Damme et al., 2007). Moreover, reduction (Boillée et al., 2006a) or ablation (Beers et al., 2006) of mutated SOD1 expression in microglia produce beneficial effects on disease duration and extend survival in $SOD1^{G93A}$ mice. We observed a reduction of astrogliosis and microgliosis in $SOD1^{G93A}Grm1^{crv4/+}$ mice, assessed by monitoring GFAP and IBA-1 expression. Due to the close relationship between neuronal and glial cells in ALS, these results, obtained by directly and indirectly decreasing mGluR1 and mGluR5 expression, support the concept that the two receptors play important roles in ALS and that this effect is not mediated exclusively by neuron.

There is evidence supporting the hypothesis that oxidative stress plays a role in MN death occurring in ALS (Lin and Beal, 2006; Robberecht, 2000). It is known that MTs and CAT are neuroprotective through their intracellular role as radical and toxic metabolite scavengers and many studies indicate that their expression/activity is altered in ALS (Babu et al., 2008; Gong and Elliott, 2000; Nikolić-Kokić et al., 2006; Ono et al., 2006). We found here that changes in MT and CAT mRNA expression, found in $SOD1^{G93A}$ mice, are restored in $SOD1^{G93A}Grm1^{crv4/+}$ mice. Interestingly, we have previously shown that administration of mesenchymal stem cells to $SOD1^{G93A}$ mice improved survival probability, slowed down disease progression and normalized the MT up-regulation (Uccelli et al., 2012), suggesting a relationship between MT mRNA expression and disease progression in $SOD1^{G93A}$ mice. Thus, both mGluR1 down regulation and mesenchymal stem cell administration, that prolong survival and ameliorate disease hallmarks, pursue normalization of oxidative stress markers, thus suggesting that this mechanism may represent a common route for disease rescue.

Mitochondrial damage, in the form of swollen/vacuolated organelles, is one feature of ongoing MN degeneration in ALS (Boillée et al., 2006a; Cozzolino and Carrì, 2012). Expression of mutant SOD1 genes is strongly associated with mitochondrial damage in both presymptomatic and symptomatic stages of SOD1 mouse models of the human pathology (Boillée et al., 2006a; Jaarsma et al., 2000, 2001). The present study confirms mitochondrial abnormalities in $SOD1^{G93A}$ mice and, most interestingly, shows that double mutant $SOD1^{G93A}Grm1^{crv4/+}$mice display lower levels of damaged mitochondria and higher levels of normal mitochondria compared to $SOD1^{G93A}$ mice. A very recent study awaiting confirmation surprisingly proposes that disease progression is not directly linked to mitochondrial damage and MN death in mutated SOD1 models (Parone et al., 2013). Even so, we believe that our findings allow us to suggest that the higher number of normal mitochondria may contribute, at least in part, to the slowdown of MN degeneration and possibly to the clinical amelioration in $SOD1^{G93A}Grm1^{crv4/+}$mice.

GLT1 is reduced in ALS and this reduction has been presumed as a major cause of excessive glutamate and excitotoxicity (Rothstein, 1995; Trotti et al., 2001). Accordingly, increase of GLT1 synthesis has been proposed as a useful therapeutic approach (Ganel et al., 2006; Rothstein et al., 2005), although recent human studies weakened this hypothesis (Cudkowicz et al., 2013). Our data shows that the decreasing mGluR1 and mGluR5 expression does not modify the amount of GLT1 in the spinal cord of $SOD1^{G93A}Grm1^{crv4/+}$ mice, thus suggesting that the mechanisms leading to amelioration of disease progression in our model are independent of the GLT1 function and are able to prevail over the possible detrimental effects of the recorded GLT1 reduction.

The core hypothesis that originated the present work is that Glu-driven excitotoxicity is sustained by abnormal mGluR1- and mGluR5-induced Glu release. We have previously observed that 3,5-DHPG induced abnormal Glu release from $SOD1^{G93A}$ mouse spinal cord synaptosomes (Giribaldi et al., 2013). In order to verify whether this abnormal release may be causally linked to the pathology, we examined the 3,5-DHPG-induced Glu release in $SOD1^{G93A}Grm1^{crv4/+}$ mice. Noteworthy, we found that mGluR1 reduction abolished the excessive release of Glu measured in $SOD1^{G93A}$ mice. Actually, Glu release, induced by 30 μM 3,5-DHPG in $SOD1^{G93A}Grm1^{crv4/+}$ and $Grm1^{crv4/+}$mice, was even significantly lower than in WT mice. We have shown that both receptors can sustain the excessive Glu release but the recruitment of mGluR5 appears to be higher when lowering the agonist concentration; the opposite is true for mGluR1. It is conceivable that genetic ablation of mGluR1 produces the release-reducing effects more efficiently when these receptors play a pivotal role, i.e. at high 3,5-DHPG concentrations. The reduction of release observed also in $Grm1^{crv4/+}$ mice, using 30 μM 3,5-DHPG, supports this hypothesis. Taken together, these results

indicate a possible link between the increase of Glu release and disease progression and suggest that the release of Glu plays a role in excitotoxicity in ALS. Clearly, Glu release is not the only cause of the pathology, since abolishing excessive release does not prevent the appearance of symptoms and death. On the other hand, abnormal release is not the only cause of excessive Glu: inhibition of astrocytic Glu uptake represents another important mechanism (Rothstein et al., 1995). These results are also in line with the notion that ALS is likely a multifactorial disease. Further studies at more precocious stages of the disease might be useful to elucidate this issue.

On the depicted ground, pharmacological treatments aimed to counteract the activity of Group I mGluRs might be beneficial in ALS. It has been shown that chronic treatment with the prototypic mGluR5 antagonist MPEP attenuates cell death, delays the onset of motor symptoms, and prolongs survival in *SOD1^{G93A}* mutant mice, although only to some extent (Rossi et al., 2008). While effective mGluR1 antagonists are only pre-clinically available at present, new, selective and potent mGluR5 antagonists are now under clinical trials. One of these, fenobam, was tested in humans for its anxiolytic and analgesic activity and in fragile X syndrome (Berry-Kravis et al., 2009; Porter et al., 2005) and exhibited a good therapeutic profile without significant adverse effects. Another compound, AFQ056, was clinically tested for Parkinson disease dyskinesia and fragile X syndrome (Berg et al., 2011; Levenga et al., 2011), again showing an attractive safety profile. Once tested in vivo in the ALS animal models these drugs may be directly translated to the clinic.

Conclusions

The present genetically-based evidence emphasizes the crucial role played by both mGluR1 and mGluR5 in determining ALS symptoms, at least in the *SOD1^{G93A}* mouse model. In fact, halving mGluR1 expression in SOD1/G93A background led to a decrease also of mGluR5. Interestingly, the reduced level of Group I mGluRs determined increased survival, amelioration of disease symptoms, MN protection from death, and improved biochemical and histological readout of disease in *SOD1^{G93A}* mice. These findings allow us to propose the excessive activity of these receptors as a novel mechanism contributing to the disease, thus providing the basis for novel pharmacological approaches to ALS by using drugs that selectively block Group I mGluRs.

Funding

This work was supported by grants from the Italian Ministero dell'Università e Ricerca (PRIN project no. 2006058401 to GB and PRIN project no. 20108WT39Y to AP), by the Ministero della Salute, Progetti Ordinari 2009 to GB, by the University of Genova (Progetto di Ateneo to AP and LV), by the Università Politecnica delle Marche (to FC) and by the Fondazione Giorgini (to FC).

Acknowledgments

The authors are grateful to Mrs. Maura Agate for her excellent secretarial assistance.

References

Andersen, P.M., Al-Chalabi, A., 2011. Clinical genetics of amyotrophic lateral sclerosis: what do we really know? Nat. Rev. Neurol. 7, 603–615.
Babu, G.N., Kumar, A., Chandra, R., Puri, S.K., Singh, R.L., Kalita, J., et al., 2008. Oxidant–antioxidant imbalance in the erythrocytes of sporadic amyotrophic lateral sclerosis patients correlates with the progression of disease. Neurochem. Int. 52, 1284–1289.
Beers, D.R., Henkel, J.S., Xiao, Q., Zhao, W., Wang, J., Yen, A.A., et al., 2006. Wild-type microglia extend survival in PU.1 knockout mice with familial amyotrophic lateral sclerosis. Proc. Natl. Acad. Sci. U. S. A. 103, 16021–16026.
Berg, D., Godau, J., Trenkwalder, C., Eggert, K., Csoti, I., Storch, A., et al., 2011. AFQ056 treatment of levodopa-induced dyskinesias: results of 2 randomized controlled trials. Mov. Disord. 26, 1243–1250.
Berry-Kravis, E., Hessl, D., Coffey, S., Hervey, C., Schneider, A., Yuhas, J., et al., 2009. A pilot open label, single dose trial of fenobam in adults with fragile X syndrome. J. Med. Genet. 46, 266–271.
Bilsland, L.G., Sahai, E., Kelly, G., Golding, M., Greensmith, L., Schiavo, G., 2010. Deficits in axonal transport precede ALS symptoms *in vivo*. Proc. Natl. Acad. Sci. U. S. A. 107, 20523–20528.
Birve, A., Neuwirth, C., Weber, M., Marklund, S.L., Nilsson, A.C., Jonsson, P.A., et al., 2010. A novel SOD1 splice site mutation associated with familial ALS revealed by SOD activity analysis. Hum. Mol. Genet. 19, 4201–4206.
Boillée, S., Vande Velde, C., Cleveland, D.W., 2006a. ALS: a disease of motor neurons and their nonneuronal neighbors. Neuron 52, 39–59.
Boillée, S., Yamanaka, K., Lobsiger, C.S., Copeland, N.G., Jenkins, N.A., Kassiotis, G., et al., 2006b. Onset and progression in inherited ALS determined by motor neurons and microglia. Science 312, 1389–1392.
Boston-Howes, W., Gibb, S.L., Williams, E.O., Pasinelli, P., Brown Jr., R.H., Trotti, D., 2006. Caspase-3 cleaves and inactivates the glutamate transporter EAAT2. J. Biol. Chem. 281, 14076–14084.
Bradford, M.M., 1976. A rapid and sensitive method for the quantitation of microgram quantities of protein utilizing the principle of protein dye binding. Anal. Biochem. 72, 248–254.
Cheah, B.C., Vucic, S., Krishnan, A.V., Kiernan, M.C., 2010. Riluzole, neuroprotection and amyotrophic lateral sclerosis. Curr. Med. Chem. 17, 1942–1959.
Cleveland, D.W., Bruijn, L.I., Wong, P.C., Marszalek, J.R., Vechio, J.D., Lee, M.K., et al., 1996. Mechanisms of selective motor neuron death in transgenic mouse models of motor neuron disease. Neurology 47 (Suppl. 2), S54–S61 (discussion S61-S62).
Conn, P.J., Pin, J.P., 1997. Pharmacology and functions of metabotropic glutamate receptors. Annu. Rev. Pharmacol. Toxicol. 37, 205–237.
Conti, F., Weinberg, R.J., 1999. Shaping excitation at glutamatergic synapses. Trends Neurosci. 22, 451–458.
Conti, V., Aghaie, A., Cilli, M., Martin, N., Caridi, G., Musante, L., et al., 2006. Crv4, a mouse model for human ataxia associated with kyphoscoliosis caused by an mRNA splicing mutation of the metabotropic glutamate receptor 1 (Grm1). Int. J. Mol. Med. 18, 593–600.
Cozzolino, M., Carrì, M.T., 2012. Mitochondrial dysfunction in ALS. Prog. Neurobiol. 97, 54–66.
Cudkowicz, M., Shefner, J., Consortium, N.E.A.L.S., 2013. STAGE 3 clinical trial of ceftriaxone in subjects with ALS (S36.001). Neurology 80, S36.001.
Damiano, M., Starkov, A.A., Petri, S., Kipiani, K., Kiaei, M., Mattiazzi, M., et al., 2006. Neural mitochondrial Ca^{2+} capacity impairment precedes the onset of motor symptoms in G93A Cu/Zn-superoxide dismutase mutant mice. J. Neurochem. 96, 1349–1361.
De Blasi, A., Conn, P.J., Pin, J., Nicoletti, F., 2001. Molecular determinants of metabotropic glutamate receptor signaling. Trends Pharmacol. Sci. 22, 114–120.
Dingledine, R., Borges, K., Bowie, D., Traynelis, S.F., 1999. The glutamate receptor ion channels. Pharmacol. Rev. 51, 7–61.
Doble, A., 1999. The role of excitotoxicity in neurodegenerative disease: implications for therapy. Pharmacol. Ther. 81, 163–221.
Dunlop, J., Beal McIlvain, H., She, Y., Howland, D.S., 2003. Impaired spinal cord glutamate transport capacity and reduced sensitivity to riluzole in a transgenic superoxide dismutase mutant rat model of amyotrophic lateral sclerosis. J. Neurosci. 23, 1688–1696.
Fazio, F., Notartomaso, S., Aronica, E., Storto, M., Battaglia, G., Vieira, E., et al., 2008. Switch in the expression of mGlu1 and mGlu5 metabotropic glutamate receptors in the cerebellum of mice developing experimental autoimmune encephalomyelitis and in autoptic cerebellar samples from patients with multiple sclerosis. Neuropharmacology 55, 491–499.
Ferraguti, F., Crepaldi, L., Nicoletti, F., 2008. Metabotropic glutamate 1 receptor: current concepts and perspectives. Pharmacol. Rev. 60, 536–581.
Ferraiuolo, L., Kirby, J., Grierson, A.J., Sendtner, M., Shaw, P.J., 2011. Molecular pathways of motor neuron injury in amyotrophic lateral sclerosis. Nat. Rev. Neurol. 7, 616–630.
Fleck, M.W., Barrionuevo, G., Palmer, A.M., 2001. Synaptosomal and vesicular accumulation of L-glutamate, L- aspartate and D-aspartate. Neurochem. Int. 39, 217–225.
Ganel, R., Ho, T., Maragakis, N.J., Jackson, M., Steiner, J.P., Rothstein, J.D., 2006. Selective up-regulation of the glial Na^{+}-dependent glutamate transporter GLT1 by a neuroimmunophilin ligand results in neuroprotection. Neurobiol. Dis. 21, 556–567.
Giribaldi, F., Milanese, M., Bonifacino, T., Rossi, P.I.A., Di Prisco, S., Pittaluga, A., et al., 2013. Group I metabotropic glutamate autoreceptors induce abnormal glutamate exocytosis in a mouse model of amyotrophic lateral sclerosis. Neuropharmacology 66, 253–263.
Gong, Y.H., Elliott, J.L., 2000. Metallothionein expression is altered in a transgenic murine model of familial amyotrophic lateral sclerosis. Exp. Neurol. 162, 27–36.
Gurney, M.E., Pu, H., Chiu, A.Y., Dal Canto, M.C., Polchow, C.Y., Alexander, D.D., et al., 1994. Motor neuron degeneration in mice that express a human Cu, Zn superoxide dismutase mutation. Science 264, 1772–1775 (Erratum in: Science 269, 149).
Heath, P.R., Shaw, P.J., 2002. Update on the glutamatergic neurotransmitter system and the role of excitotoxicity in amyotrophic lateral sclerosis. Muscle Nerve 26, 438–458.
Howland, D.S., Liu, J., She, Y., Goad, B., Maragakis, N.J., Kim, B., et al., 2002. Focal loss of the glutamate transporter EAAT2 in a transgenic rat model of SOD1 mutant-mediated amyotrophic lateral sclerosis (ALS). Proc. Natl. Acad. Sci. U. S. A. 99, 1604–1609.
Ilieva, H., Polymenidou, M., Cleveland, D.W., 2009. Non-cell autonomous toxicity in neurodegenerative disorders: ALS and beyond. J. Cell Biol. 187, 761–772.
Jaarsma, D., Haasdijk, E.D., Grashorn, J.A., Hawkins, R., van Duijn, W., Verspaget, H.W., et al., 2000. Human Cu/Zn superoxide dismutase (SOD1) overexpression in mice causes mitochondrial vacuolization, axonal degeneration, and premature motoneuron death and accelerates motoneuron disease in mice expressing a familial amyotrophic lateral sclerosis mutant SOD1. Neurobiol. Dis. 7 (6 Pt B), 623–643.
Jaarsma, D., Rognoni, F., van Duijn, W., Verspaget, H.W., Haasdijk, E.D., Holstege, J.C., 2001. CuZn superoxide dismutase (SOD1) accumulates in vacuolated mitochondria in

transgenic mice expressing amyotrophic lateral sclerosis-linked SOD1 mutations. Acta Neuropathol. 102, 293–305.
Lanza, C., Morando, S., Voci, A., Canesi, L., Principato, M.C., Serpero, L.D., et al., 2009. Neuroprotective mesenchymal stem cells are endowed with a potent antioxidant effect *in vivo*. J. Neurochem. 110, 1674–1684.
Lasiene, J., Yamanaka, K., 2011. Glial cells in amyotrophic lateral sclerosis. Neurol. Res. Int. 718987.
Levenga, J., Hayashi, S., de Vrij, F.M., Koekkoek, S.K., van der Linde, H.C., Nieuwenhuizen, I., et al., 2011. AFQ056, a new mGluR5 antagonist for treatment of fragile X syndrome. Neurobiol. Dis. 42, 311–317.
Li, Q., Spencer, N.Y., Pantazis, N.J., Engelhardt, J.F., 2011. Alsin and SOD1(G93A) proteins regulate endosomal reactive oxygen species production by glial cells and proinflammatory pathways responsible for neurotoxicity. J. Biol. Chem. 286, 40151–40162.
Lin, M.T., Beal, M.F., 2006. Mitochondrial dysfunction and oxidative stress in neurodegenerative diseases. Nature 443, 787–795.
Milanese, M., Zappettini, S., Jacchetti, E., Bonifacino, T., Cervetto, C., Usai, C., et al., 2010. In vitro activation of GAT1 transporters expressed in spinal cord gliosomes stimulates glutamate release that is abnormally elevated in the SOD1/G93A(+) mouse model of amyotrophic lateral sclerosis. J. Neurochem. 113, 489–501.
Milanese, M., Zappettini, S., Onofri, F., Musazzi, L., Tardito, D., Bonifacino, T., et al., 2011. Abnormal exocytotic release of glutamate in a mouse model of amyotrophic lateral sclerosis. J. Neurochem. 116, 1028–1042.
Nicoletti, F., Bockaert, J., Collingridge, G.L., Conn, P.J., Ferraguti, F., Schoepp, D.D., et al., 2011. Metabotropic glutamate receptors: from the workbench to the bedside. Neuropharmacology 60, 1017–1041.
Nikolić-Kokić, A., Stević, Z., Blagojević, D., Davidović, B., Jones, D.R., Spasić, M.B., 2006. Alterations in anti-oxidative defence enzymes in erythrocytes from sporadic amyotrophic lateral sclerosis (SALS) and familial ALS patients. Clin. Chem. Lab. Med. 44, 589–593.
Ono, S., Endo, Y., Tokuda, E., Ishige, K., Tabata, K., Asami, S., et al., 2006. Upregulation of metallothionein-I mRNA expression in a rodent model for amyotrophic lateral sclerosis. Biol. Trace Elem. Res. 113, 93–104.
Parone, P.A., Da Cruz, S., Han, J.S., McAlonis-Downes, M., Vetto, A.P., Lee, S.K., et al., 2013. Enhancing mitochondrial calcium buffering capacity reduces aggregation of misfolded SOD1 and motor neuron cell death without extending survival in mouse models of inherited amyotrophic lateral sclerosis. J. Neurosci. 33, 4657–4671.
Perry, T.L., Krieger, C., Hansen, S., Eisen, A., 1990. Amyotrophic lateral sclerosis: amino acid levels in plasma and cerebrospinal fluid. Ann. Neurol. 28, 12–17.
Porter, R.H., Jaeschke, G., Spooren, W., Ballard, T.M., Büttelmann, B., Kolczewski, S., et al., 2005. Fenobam: a clinically validated nonbenzodiazepine anxiolytic is a potent, selective, and noncompetitive mGlu5 receptor antagonist with inverse agonist activity. J. Pharmacol. Exp. Ther. 315, 711–721.
Raiteri, M., Bonanno, G., Marchi, M., Maura, G., 1984. Is there a functional linkage between neurotransmitter uptake mechanisms and presynaptic receptors? J. Pharmacol. Exp. Ther. 231, 671–677.
Raiteri, L., Paolucci, E., Prisco, S., Raiteri, M., Bonanno, G., 2003. Activation of a glycine transporter on spinal cord neurons causes enhanced glutamate release in a mouse model of amyotrophic lateral sclerosis. Br. J. Pharmacol. 138, 1021–1025.
Raiteri, L., Stigliani, S., Zappettini, S., Mercuri, N.B., Raiteri, M., Bonanno, G., 2004. Excessive and precocious glutamate release in a mouse model of amyotrophic lateral sclerosis. Neuropharmacology 46, 782–792.
Robberecht, W., 2000. Oxidative stress in amyotrophic lateral sclerosis. J. Neurol. 247 (Suppl. 1), I1–I6.
Rosen, D.R., Siddique, T., Patterson, D., Figlewicz, D.A., Sapp, P., Hentati, A., et al., 1993. Mutations in Cu/Zn superoxide dismutase gene are associated with familial amyotrophic lateral sclerosis. Nature 364, 59–62.
Rossi, D., Brambilla, L., Valori, C.F., Roncoroni, C., Crugnola, A., Yokota, T., et al., 2008. Focal degeneration of astrocytes in amyotrophic lateral sclerosis. Cell Death Differ. 15, 1691–1700.
Rossi, P.I., Musante, I., Summa, M., Pittaluga, A., Emionite, L., Ikehata, M., et al., 2012. Compensatory molecular and functional mechanisms in nervous system of the Grm1crv4 mouse lacking the mGlu1 receptor: a model for motor coordination deficits. Cereb. Cortex 23 (9), 2179–2189.
Rothstein, J.D., 1995. Excitotoxicity and neurodegeneration in amyotrophic lateral sclerosis. Clin. Neurosci. 3, 348–359.
Rothstein, J.D., Martin, L.J., Kuncl, R.W., 1992. Decreased glutamate transport by the brain and spinal cord in amyotrophic lateral sclerosis. N. Engl. J. Med. 326, 1464–1468.
Rothstein, J.D., Van Kammen, M., Levey, A.I., Martin, L.J., Kuncl, R.W., 1995. Selective loss of glial glutamate transporter GLT-1 in amyotrophic lateral sclerosis. Ann. Neurol. 38, 73–84.
Rothstein, J.D., Patel, S., Regan, M.R., Haenggeli, C., Huang, Y.H., Bergles, D.E., et al., 2005. Beta-lactam antibiotics offer neuroprotection by increasing glutamate transporter expression. Nature 433, 73–77.
Sasaki, S., Warita, H., Murakami, T., Abe, K., Iwata, M., 2004. Ultrastructural study of mitochondria in the spinal cord of transgenic mice with a G93A mutant SOD1 gene. Acta Neuropathol. 107, 461–474.
Shaw, P.J., Eggett, C.J., 2000. Molecular factors underlying selective vulnerability of motor neurons to neurodegeneration in amyotrophic lateral sclerosis. J. Neurol. 247 (Suppl. 1), I17–I27.
Stifanese, R., Averna, M., De Tullio, R., Pedrazzi, M., Beccaria, F., Salamino, F., et al., 2010. Adaptive modifications in the calpain/calpastatin system in brain cells after persistent alteration in Ca^{2+} homeostasis. J. Biol. Chem. 285, 631–643.
Tortarolo, M., Grignaschi, G., Calvaresi, N., Zennaro, E., Spaltro, G., Colovic, M., et al., 2006. Glutamate AMPA receptors change in motor neurons of SOD1G93A transgenic mice and their inhibition by a noncompetitive antagonist ameliorates the progression of amyotrophic lateral sclerosis-like disease. J. Neurosci. Res. 83, 134–146.
Trotti, D., Aoki, M., Pasinelli, P., Berger, U.V., Danbolt, N.C., Brown Jr., R.H., et al., 2001. Amyotrophic lateral sclerosis-linked glutamate transporter mutant has impaired glutamate clearance capacity. J. Biol. Chem. 276, 576–582.
Uccelli, A., Milanese, M., Principato, M.C., Morando, S., Bonifacino, T., Vergani, L., et al., 2012. Intravenous mesenchymal stem cells improve survival and motor function in experimental amyotrophic lateral sclerosis. Mol. Med. 18, 794–804.
Van Damme, P., Bogaert, E., Dewil, M., Hersmus, N., Kiraly, D., Scheveneels, W., et al., 2007. Astrocytes regulate GluR2 expression in motor neurons and their vulnerability to excitotoxicity. Proc. Natl. Acad. Sci. U. S. A. 104, 14825–14830.
Wang, L., Gutmann, D.H., Roos, R.P., 2011a. Astrocyte loss of mutant SOD1 delays ALS disease onset and progression in G85R transgenic mice. Hum. Mol. Genet. 20, 286–293.
Wang, L., Popko, B., Roos, R.P., 2011b. The unfolded protein response in familial amyotrophic lateral sclerosis. Hum. Mol. Genet. 20, 1008–1015.
Watson, C., Paxinos, G., Kayalioglu, G., 2008. The Spinal Cord. Academic Press, Amsterdam.
Yamanaka, K., Chun, S.J., Boillee, S., Fujimori-Tonou, N., Yamashita, H., Gutmann, D.H., et al., 2008. Astrocytes as determinants of disease progression in inherited amyotrophic lateral sclerosis. Nat. Neurosci. 11, 251–253.